



**HAL**  
open science

# New mathematical methods in analysis of High Resolution Electrocardiography Mapping

Balkine Khaddoumi, Hervé Rix, Malgorzata Fereniec

► **To cite this version:**

Balkine Khaddoumi, Hervé Rix, Malgorzata Fereniec. New mathematical methods in analysis of High Resolution Electrocardiography Mapping. High Resolution ECG Mapping, Nov 2007, Varsovie, Poland. pp 9-15. hal-00368514

**HAL Id: hal-00368514**

**<https://hal.science/hal-00368514>**

Submitted on 16 Mar 2009

**HAL** is a multi-disciplinary open access archive for the deposit and dissemination of scientific research documents, whether they are published or not. The documents may come from teaching and research institutions in France or abroad, or from public or private research centers.

L'archive ouverte pluridisciplinaire **HAL**, est destinée au dépôt et à la diffusion de documents scientifiques de niveau recherche, publiés ou non, émanant des établissements d'enseignement et de recherche français ou étrangers, des laboratoires publics ou privés.

# NEW MATHEMATICAL METHODS IN ANALYSIS OF HIGH RESOLUTION ELECTROCARDIOGRAHY MAPPING

B. Khaddoumi<sup>\*</sup>, H. Rix<sup>\*\*</sup>, M. Fereniec<sup>\*\*\*</sup>

<sup>\*</sup> Ecole Supérieure des Sciences de Tunis, Tunisia

<sup>\*\*</sup> University Nice-Sophia Antipolis & CNRS, Sophia Antipolis, France

<sup>\*\*\*</sup> Institute of Biocybernetics and Biomedical Engineering, PAS, Warsaw, Poland

## Abstract

Recent mathematical methods, dealing with shape analysis and shape clustering are presented. The advantage of taking signal shape into account is shown in an application to High Resolution ECG Mapping: the spatial dispersion of the ECG waves recorded with a 64 lead device, and mainly the T-wave, is well correlated with the presence of Myocardial Infarcts.

## 1. Introduction

High resolution electrocardiography (HR ECG) and body surface potential mapping (BSPM) are non-invasive methods used for evaluation of electric activity of the heart. In this paper we demonstrate the usefulness of a 64-lead high-resolution ECG measurement, combined with shape analysis (SA), for providing pertinent information from the ECG. The aim of the paper is to show, that the spatial variability of ECG waves can be significantly estimated and may assess departures from the healthy state. In particular, in the case of MI patients threatened by ventricular arrhythmia compared to healthy subjects, the presence of a necrosis generates local alterations of the myocardium, leading to inhomogeneous repolarization. So we could expect to observe an increased spatial variability of the shapes, on T-waves, at the body surface.

The examination was carried out in the electrically shielded room using the high-resolution ECG measurement system. The system consists of 64 low noise amplifiers with 16-bit A/D converters (BIOSEMI, the Netherlands). Digital signals were transformed to the serial optical format and then were transferred to the computer via an optical fiber. The data acquisition was controlled by the LabView measurement software. To improve the signal-to-noise ratio the cross-correlation averaging and filtering methods were applied to 64 signals obtained from the lead position on the torso according to the University of Amsterdam lead system

## 2. Theory

Before using the notion of signal shape in signal processing, we have first to define shape equality, then to provide a measure of shape difference and finally to show how to make statistics on shapes.

### 2.1. Shape equality

A shape is, for us, a class of equivalence of signals. The equivalence is associated to the affine group acting both on the left and on the right of the set of signals we are interested in. Thus,

signals  $s(t)$  and  $v(t)$  are the same shape if and only if they are linked by:

$$v(t) = ks(\alpha t + t_0) + C \quad \alpha > 0, k > 0 \quad (1)$$

In the application to ECG, the baseline is subtracted. Therefore we will assume  $C = 0$  and equation (1) will be replaced by:

$$v(t) = ks(\alpha t + t_0) \quad \alpha > 0, k > 0 \quad (2) \quad \text{which is equivalent to:}$$

$$s(t') = k' v\left(\frac{t' - t_0}{\alpha}\right), \quad \text{where } t' = \alpha t + t_0 \text{ and } k' = \frac{1}{k} \quad (3)$$

## 2.2. Shape difference of positive signals

The signals are assumed to be positive on their supports: they represent either the recorded signals or positive function of them, like the square or the absolute value. The technique we used is called the Distribution Function Method (DFM) [4]. Let us define the normalized integrals  $S(t)$  and  $V(t)$  of  $s(t)$  and  $v(t)$  respectively,  $[a, b]$  and  $[c, d]$  being their respective supports:

$$S(t) = \frac{\int_a^t s(\tau) d\tau}{\int_a^b s(\tau) d\tau} \quad ; \quad V(t) = \frac{\int_c^t v(\tau) d\tau}{\int_c^d v(\tau) d\tau} \quad (4)$$

$s(t)$  and  $v(t)$  being positive,  $S(t)$  and  $V(t)$  are increasing functions (on the supports of  $s(t)$  and  $v(t)$  respectively) which can be linked by an increasing function  $\varphi(t)$ , modeling the change in shape between the two signals :

$$V(t) = S(\varphi(t)) \Leftrightarrow \varphi(t) = S^{-1}(V(t)) \quad (5)$$

$$\text{i.e. } \varphi = S^{-1} \circ V \quad \text{or} \quad \varphi^{-1} = V^{-1} \circ S$$

Practically, in the numerical form, the interval  $[0, 1]$  is sampled by  $M$  equidistant values  $y_i$ :

$0 < y_i < 1 \quad i = 1 \text{ to } M$ . Solving (using e.g. linear interpolation) the equation:

$$y_i = S(t_i) = V(t'_i) \quad (6)$$

gives a set of couples  $(t_i, t'_i)$  linked by  $t'_i = \varphi(t_i)$ . In case of equal shape signals, i.e. if equation (2) is true,  $\varphi(t) = \alpha t + t_0$ . The departure of function  $\varphi$  from linearity measures the shape difference. For example, fitting the least mean square line to the data  $(t_i, t'_i)$ , the root mean square of the residue may be such a measure.

## 2.3. Averaging signals

If we want to make shape clustering, i.e. to cluster the signals according to their shapes, we need an averaging technique in addition to the possibility of measuring shape differences. The

first constraint imposed to such a technique is to preserve shape when averaging equal shape signals. In the following, we show that the classical signal averaging is not a good candidate and then recall Integral Shape Averaging (ISA) and Corrected Integral Shape Averaging (CISA).

### 2.3.1 Classical Signal Averaging

#### \* Ideal case

This technique, also known as ensemble averaging is well fitted no noise reduction when the following hypotheses hold: equal shape, equal width and perfectly aligned signals. In addition the zero mean added noise and the signals are assumed to be independent. So, the signals to average can be modeled as:

$$x_i(t) = k_i s(t) + n_i(t) \quad (7)$$

$$i = 1 \text{ to } N, n_i(t) = \text{zero mean noise}$$

$$\bar{x}(t) = \frac{1}{N} \sum_{i=1}^N x_i(t) = \bar{k}s(t) + \bar{n}(t) \approx \bar{k}s(t) \quad (8)$$

So, for N sufficiently large and assuming the hypotheses, signal average gives a good estimate of s(t) within an amplitude factor. In the following this factor will be taken equal to 1.

#### \* With jitter

When the alignment process is not able to completely suppress all the jittering effect, the model becomes:

$$x_i(t) = k_i s(t - d_i) + n_i(t) \quad i = 1 \text{ to } N \quad (9)$$

When N goes to infinity, the arithmetic average does not estimate the signal s(t) but its convolution with the probability density function (pdf) of the random delay:

$$\bar{x}(t) = s * f_D(t) \quad (10)$$

#### \* With jitter and scale fluctuations

Another drawback of the classical signal averaging technique, which is never mentioned in any alignment process, is the possibility, even if shape can be assumed constant, of fluctuations of the duration of the signals, modeled by time-scale fluctuations. Let us model these fluctuations, according to:

$$x_i(t) = k_i s(\alpha_i t - d_i) + n_i(t) \quad i = 1 \text{ to } N \quad (11)$$

It has been shown [5], assuming  $\alpha_i$  is a realisation of the random variable A, independent of the delay D, that (10) must be relaced by:

$$\bar{x}(t) = \frac{1}{t} \int_0^{\infty} f_A\left(\frac{t}{\tau}\right) (s * f_D)(\tau) d\tau \quad (12)$$

Equation (12), where  $f_A$  is the pdf of the random variable A, means that signal averaging can be viewed as a linear time-shift invariant filter followed by a linear time-scale invariant filter [5]. Each filter modifies the shape of the signal.

### 2.3.2 Integral Shape Averaging (ISA)

Let  $s_i(t)$ ,  $i = 1$  to  $N$ , be  $N$  positive signals and  $S_i(t)$  their normalized integrals. The ISA signal is defined [5, 6] by the inverse of its normalized integral:

$$\tilde{S}^{-1}(y) = \frac{1}{N} \sum_{i=1}^N S_i^{-1}(y) \quad 0 \leq y \leq 1 \quad (13)$$

The ISA signal is:

$$\tilde{s}(t) = \frac{d}{dt} \tilde{S}(t) \quad (14)$$

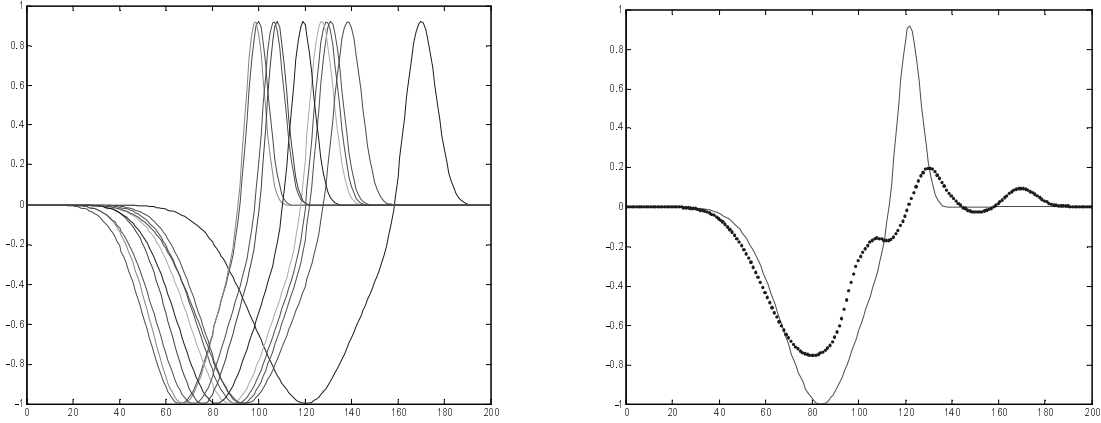


Fig. 1. Illustration of Integral Shape Averaging. The signals on the left are shifted and scaled versions of the same signal; on the right this signal is completely recovered by ISA; the classical averaged signal is given for comparison.

When all the signals  $s_i(t)$  are the same shape, i.e. they are all shifted and scaled versions of the same signal, the interesting property of ISA is to give a mean signal with the same shape, shifted and scaled by the average delay and the average scale respectively. In this case, the shape of the ISA signal is invariant through affine transforms of the signals to average.

An illustration of ISA is given in Fig. 1. In this example the positive and the negative parts of the signals are processed separately.

In the case of signals  $s_i(t)$  with different shapes, ISA still provides a mean signal, but the invariance property for the affine group is not true. The algorithm of Corrected Integral Shape Averaging (CISA), proposed in [7], makes it possible to extract an average shape from any set of signals.

### 2.3.3 Corrected Integral Shape Averaging

Let us call  $\Gamma_{CISA}$  the normalized integral of the CISA signal  $\gamma_{CISA}$ . Each  $S_i$  can be linked to  $\Gamma_{CISA}$  by an increasing function:

$$S_i(t) = \Gamma_{CISA}(\varphi_i(t)) \quad (15)$$

To separate affine transformations from shape distortion, the function  $\varphi_i$  is modeled as:

$$\begin{aligned}
\varphi_i(t) &= v_i(A_i(t)) \\
v_i(t) &= t + m_i(t) \\
\omega_i(t) &= v_i^{-1}(t) = t + n_i(t) \\
A_i(t) &= \alpha_i t + \beta_i \quad \alpha_i > 0
\end{aligned} \tag{16}$$

The CISA signal is obtained by a minimization algorithm using the distance defined below.

$$d_{CISA}(s_1, s_2) = \left[ \int_0^1 ((n_1 - n_2) \circ \Gamma_{CISA}^{-1}(y))^2 dy \right]^{1/2} \tag{17}$$

The distance between  $s_1$  and  $s_2$  is null if the non linear distortions  $n_1$  and  $n_2$  are the same.

$$\arg \min_{\mu} \sum_{i=1}^N d_{CISA}^2(\mu, s_i) = \frac{d}{dt} \left[ \left( \frac{1}{N} \sum_{i=1}^N A_i \circ S_i^{-1} \right)^{-1} \right] = \mathcal{Y}_{CISA} \tag{18}$$

For more details on the algorithm, see [7].

### 3. Application to High Resolution ECG Mapping

Shape analysis has been applied to the ECG waves recorded from a BSPM device of 64 leads. The aim was to link the spatial variability of some ECG wave, mainly the T-wave, to the presence of a myocardial infarct (MI) in patients with or without implanted cardioverter defibrillator (ICD). The application of the tools described in section 2 has been published with a first set of healthy and MI patients without ICD in [8]. In this paper we recall the principle of the procedure and the results of the application to ICD patients.

#### 3.1 Procedure

In each column of leads, each lead is associated to the absolute value of an average wave (in order to work on positive signals). The ISA signal is computed in each column and the shape dispersion is measured by the mean shape difference of each lead in the column, using DFM, to this ISA signal. This reference is probably suboptimal, comparing to CISA, but the difference is slight and the computing time is significantly shorter with ISA.

#### 3.2 Results

In Fig. 2, the shape dispersion averaged on each set of subjects, is shown column by column, for each ECG wave. The difference between the upper curve (non healthy) and the lower (healthy) is obvious for the T wave and specially in the precordial region.

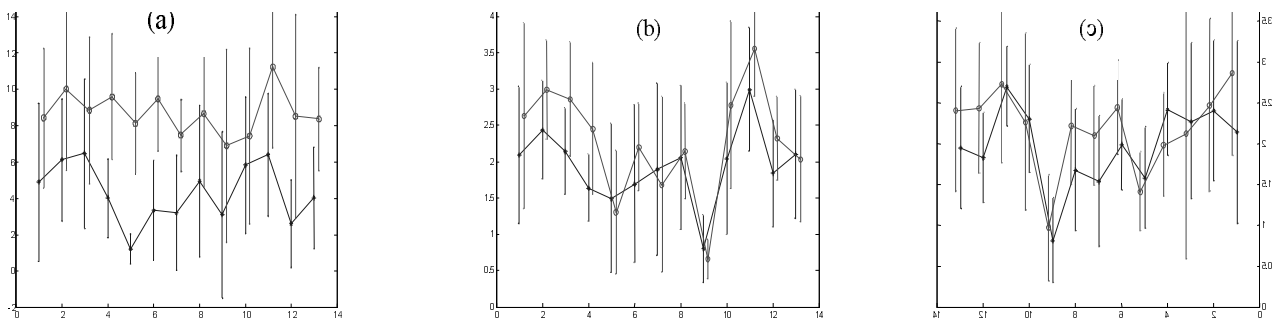


Fig. 2. Shape dispersion using ISA as the reference in each column (a) T-Waves, (b) QRS Complexes, (c) P-Waves from [Khaddoumi et al. 2006]

In order to show the clustering power of shape dispersion, we applied the Karhunen-Loève Transform to the two populations. The data were vectors  $X_p$  (associated to each person  $p$ ) of 61 components (number of active electrodes) representing the shape difference between the ECG wave recorded at the corresponding lead and the ISA Signal of its column. Let us call  $V_1$  (respectively  $V_2$ ) the main eigen vector of the healthy group (respectively the patient group),  $a_1(p)$  (respectively  $a_2(p)$ ) the scalar product of  $X_p$  with  $V_1$  (respectively  $V_2$ ). The discriminant parameter for the clustering was:

$$d(p) = a_1(p) - a_2(p)$$

The results, using T-wave shape dispersion from our first data [9], have been confirmed by new data containing patients with ICD. In Fig. 3, as expected, the index  $d(p)$  is positive (except for one) for the healthy group and negative (except for three) for the patient group.

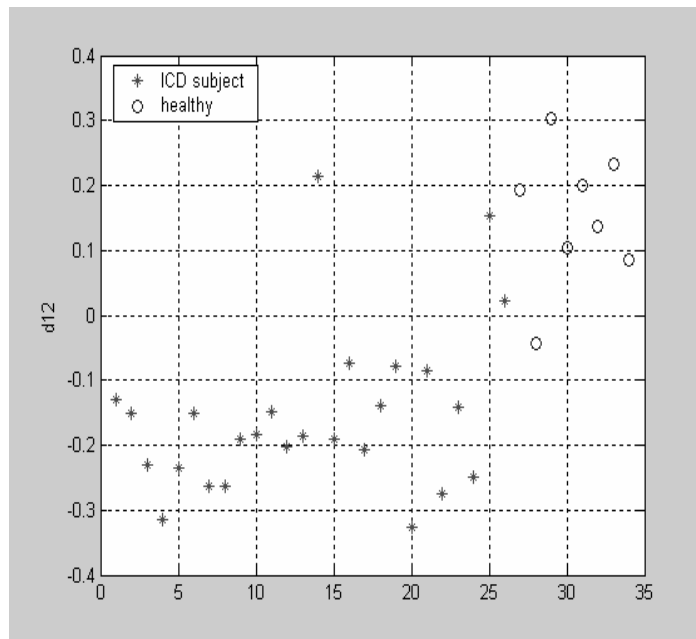


Fig. 3. Clustering with T-wave shape. The index  $d(p)$  for the patient group (on the left) and the healthy group (on the right)

#### 4. Conclusion

The presented results show that High Resolution ECG Mapping, associated to signal shape analysis using tools fitted to statistics on shapes, makes it possible to extract valuable information from spatial dispersion of the ECG waveforms. Further works, including more data, will attempt to cluster MI patients with ICD (i.e. having an history of tachycardia or ventricular fibrillation) from MI patients without ICD.

#### References

1. Hubley-Kozey C., Mitchell L., Gardner M., Warren J., Penny C., Smith E., and Horacek B.: Spatial features in Body-Surface Potential Maps can identify patients with a history of sustained ventricular tachycardia; *Circulation*, 1995, 92, 1825-38.
2. Flowers N., and Horan L.: Body surface potential mapping; In: D. Zipes and J. Jalife, eds., *Cardiac electrophysiology. From cell to bedside*. Philadelphia, Pa: WB: Saunders, 1995, 1049-67.
3. Bailon R., Olmos S., Horacek B., and Laguna P.: Identification of patient at risk for ventricular tachycardia by means of Body Surface Potential Maps; *Computers in Cardiology*, 2003, 30, 217-20.
4. Rix H., and Malengé J.P.: Detecting small variations in shape; *IEEE Trans. Syst., Man. & Cybern.*, 1980, 10, 90-96.
5. Rix H., Meste O., and Muhammad W.: Averaging Signal with Random Time Shift and Time Scale Fluctuations; *Methods of Information in Medicine*, 2004, 43, 13-16.
6. Boudaoud S., Rix H., and MESTE O.: Integral Shape Averaging and Structural Average Estimation: A Comparative Study; *IEEE Trans. Signal Processing*, 2005, 53, 3644-50.
7. Boudaoud S., Rix H., Meste O., Heneghan C., and O'Brien C.: Corrected Integral Shape Averaging applied to Obstructive Sleep Apnoea detection from the Electrocardiogram; *EURASIP Journal on Advances in Signal Processing*, Special issue on *Advances in Electrocardiogram Signal Processing and Analysis*, 2007, Article ID 32570, 12 pages, doi:10.1155/2007/32750.
8. Khaddoumi B., Rix H., Meste O., Fereniec M., Maniewski R. : Body Surface ECG Signal Shape Dispersion; *IEEE Trans. Biomed. Eng.*, 2006, 53, 2491-2500.
9. Khaddoumi B., Rix H., Meste O., Fereniec M., and Maniewski R.: Spatial shape variability of ECG waves; *The 3<sup>rd</sup> European Medical and Biological Engineering Conference, EMBC'05*, 2005, CD-ROM, 4 pages. Prague, Czech Republic.

Address for correspondence.

Hervé Rix  
Laboratoire I3S, Université de Nice-Sophia Antipolis & CNRS,  
Les Algorithmes, Euclide-B, 2000 Rte des Lucioles, BP 121,  
06903 Sophia Antipolis, France  
Email: [rix@i3s.unice.fr](mailto:rix@i3s.unice.fr)